Supplemental material

Kadakia et al., https://doi.org/10.1084/jem.20182285

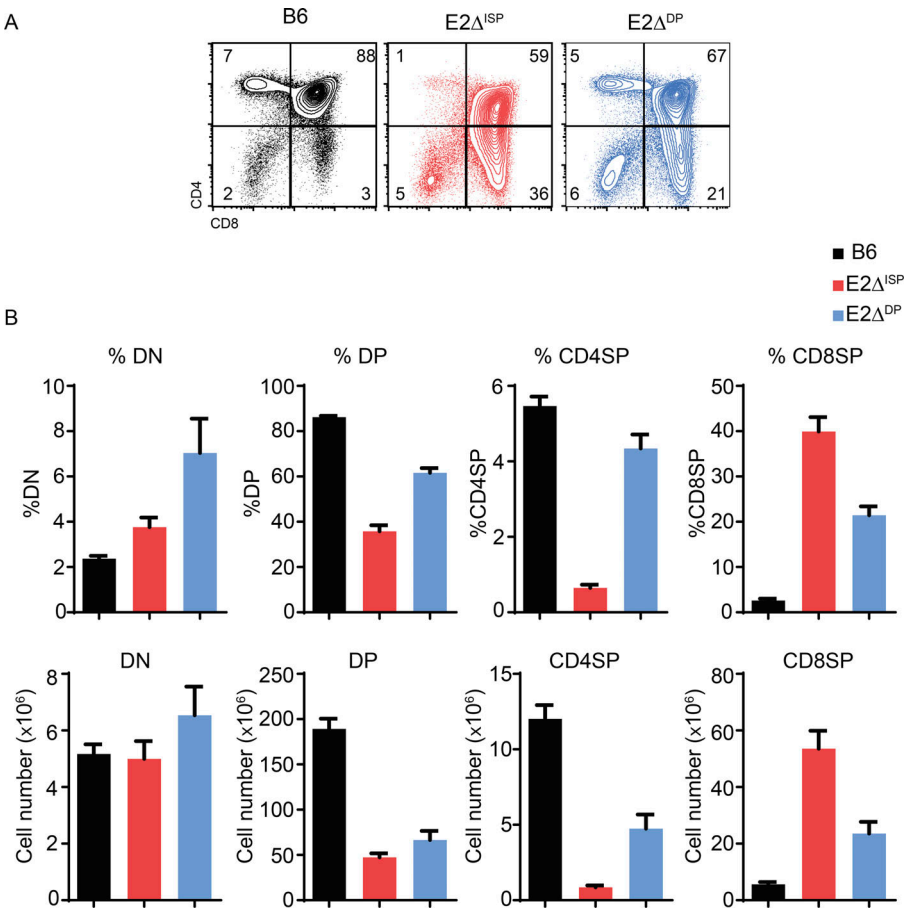

Figure S1. **Characterization of thymocytes from wild-type and E2A/HEB-deficient mice. (A)** CD4/CD8 thymocytes profiles from B6, E2Δ^{ISP}, and E2Δ^{DP} mice. Numbers in the histograms indicate the frequency of the indicated population. **(B)** Bar graphs display frequencies (top) and cell numbers (bottom) of various thymocyte subsets in the indicated mice. Data are from 3–20 experiments with 12–22 mice per group. Mean ± SEM are shown.

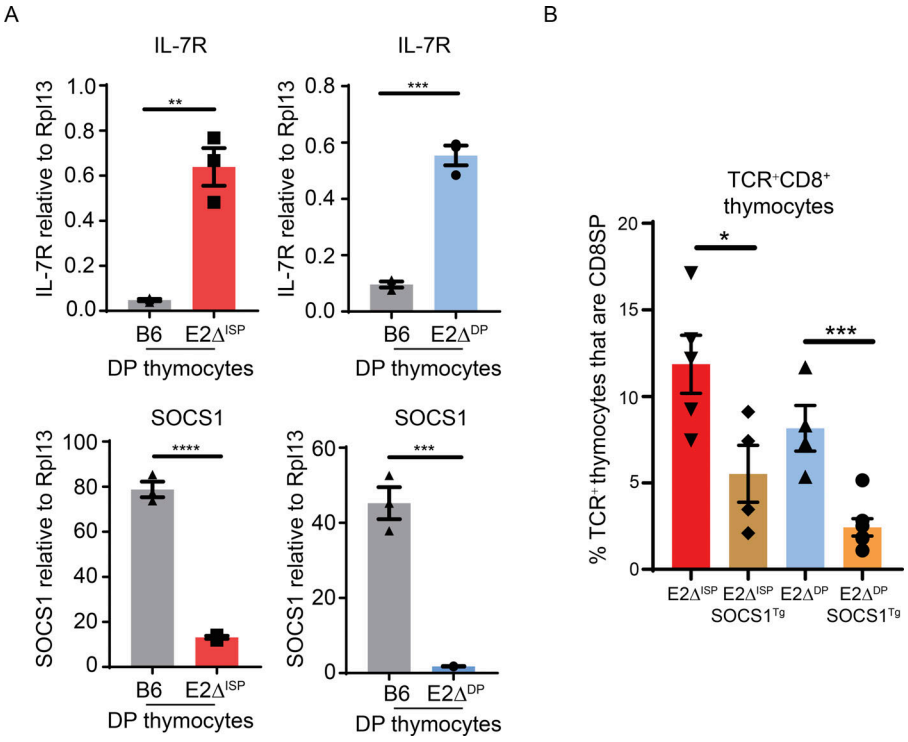

Figure S2. **E2A/HEB-deficient DP thymocytes acquire cytokine responsiveness by up-regulating IL-7R and extinguishing SOCS1 expression. (A)** IL-7R and SOCS1 mRNA in electronically sorted DP thymocytes from B6, E2Δ^{ISP}, and E2Δ^{DP} mice. Whereas all DP thymocytes in E2Δ^{ISP} mice had deleted E2A and HEB, we specifically sorted on the CXCR4^{-} subset of DP thymocytes in E2Δ^{DP} mice because these had deleted E2A and HEB. **(B)** Impact of SOCS1^{Tg} expression on frequencies of TCRβ^{+}CD8^{+} thymocytes in E2Δ^{ISP} and E2Δ^{DP} mice. Data are representative of two independent experiments (A) and are from 3–12 experiments with three to seven mice per group (B). Mean ± SEM are shown. *, P < 0.05; **, P < 0.01; ***, P < 0.001; ****, P < 0.0001 determined by Student's *t* test.

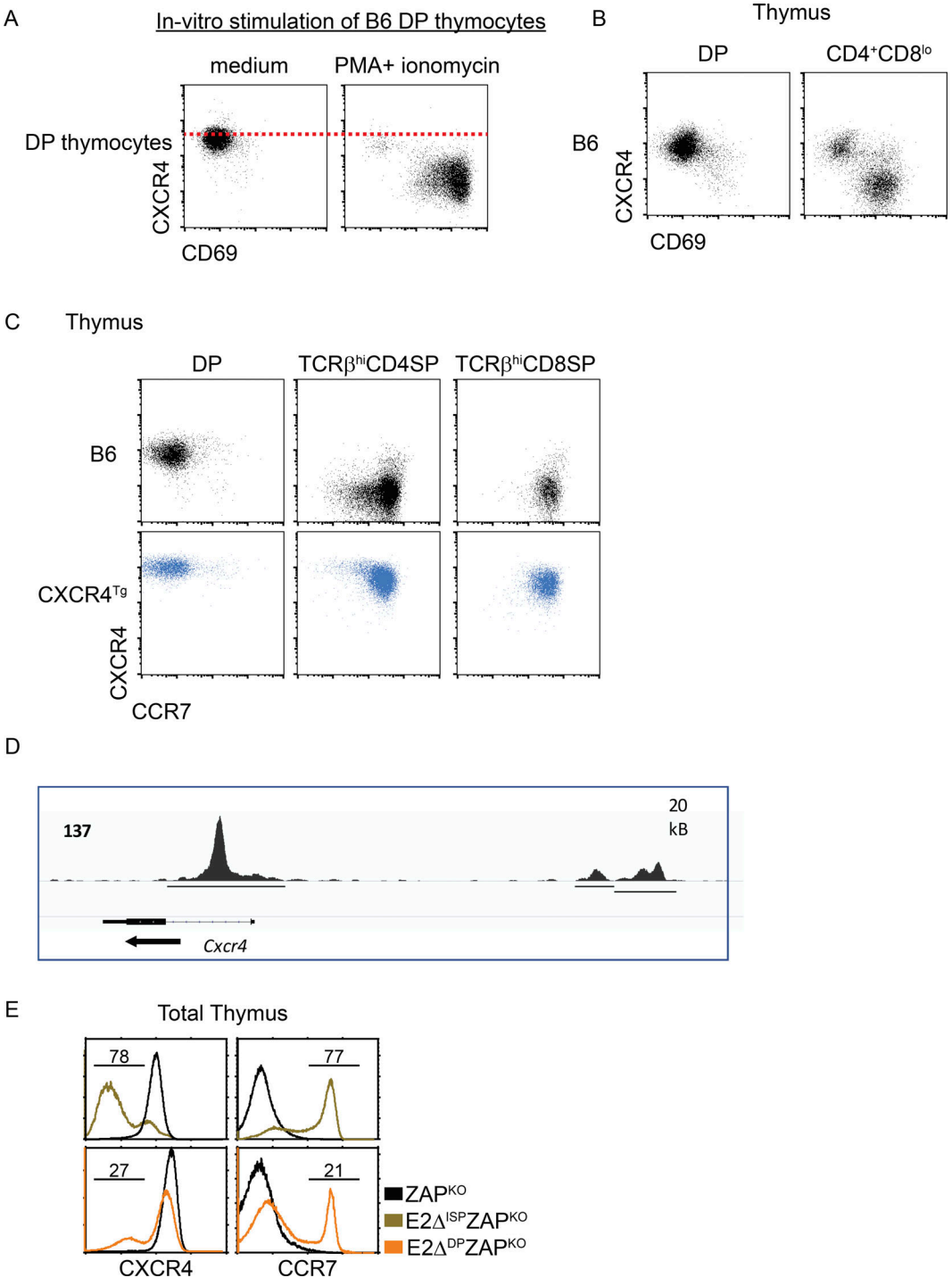

Figure S3. **CXCR4 expression is extinguished on TCR-signaled thymocytes. (A)** Flow cytometric analysis showing CXCR4 versus CD69 staining of B6 DP thymocytes that were cultured overnight in medium alone or stimulated with PMA+ ionomycin to mimic TCR signaling. Thymocytes receiving TCR signals up-regulate CD69 but extinguish CXCR4 expression. **(B)** CXCR4/CD69 profiles on DP thymocytes and postselection $CD4^+CD8^{Lo}$ thymocytes from B6 mice. **(C)** CXCR4 versus CCR7 profiles on preselection DP and postselection $TCR\beta^{hi}CD4^+$ and $TCR\beta^{hi}CD8^+$ thymocytes from B6 and $CXCR4^{Tg}$ mice. **(D)** E2A ChIP peaks at the CXCR4 promoter in DP thymocytes. Length of the genome is indicated on the top right. Numbers at the top of the track indicate maximum peak height. **(E)** E-protein deletion down-regulates CXCR4 and up-regulates CCR7 expression on TCR-unsignaled thymocytes in ZAP^{KO} mice. Overlays of CCR7 expression on thymocytes from E-protein–sufficient and E-protein–deficient ZAP^{KO} mice. Numbers indicate frequencies of $CXCR4^-$ and $CCR7^+$ thymocytes in the indicated mice. Note that a minority of thymocytes in $E2\Delta^{DP}ZAP^{KO}$ have deleted E-proteins, because most DP thymocytes arise before $E8_{III}$-Cre–mediated deletion occurs. Data are from ≤16 experiments with 3–23 mice per group.

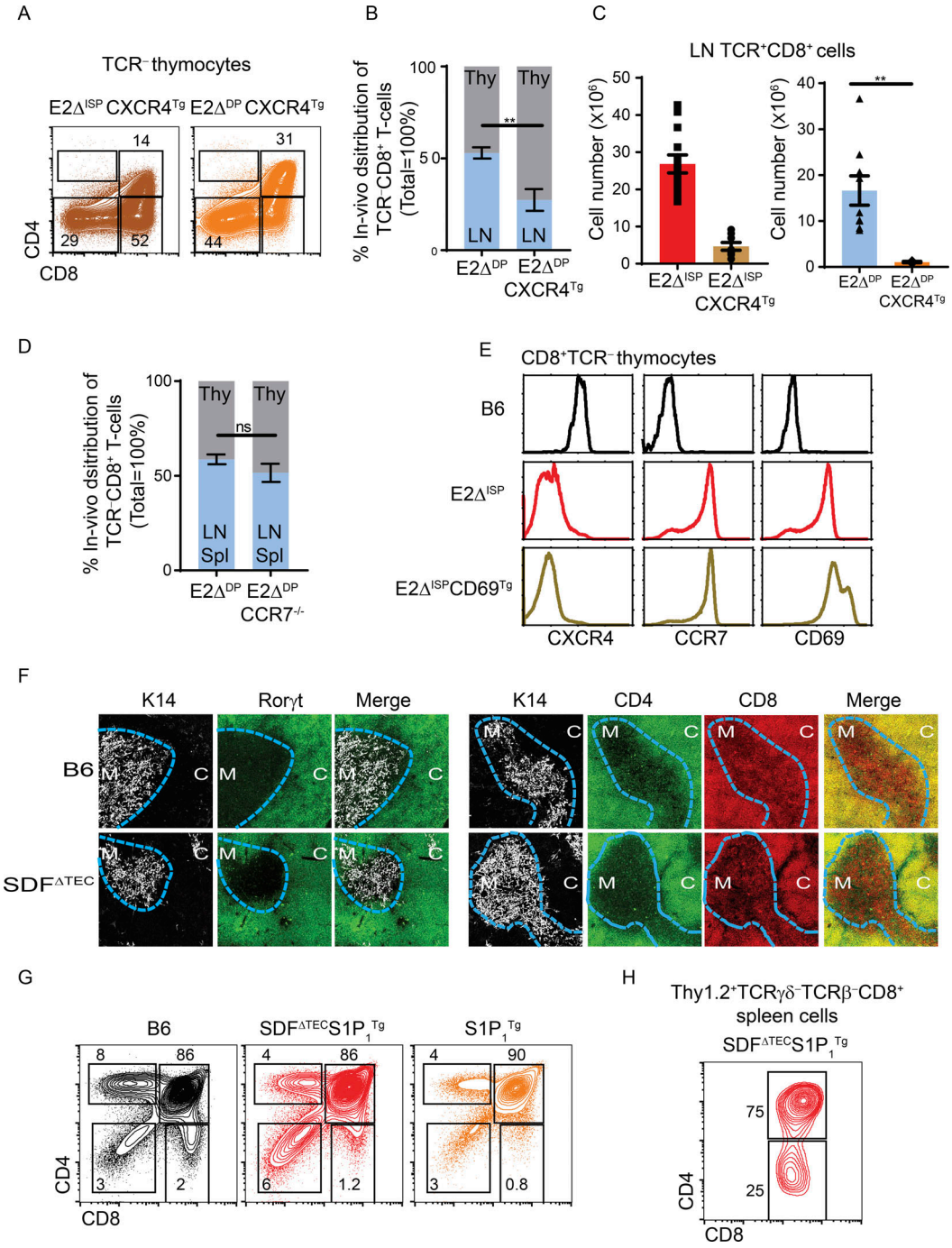

Figure S4. **Interaction of CXCR4 with its ligand CXCL12 (SDF-1) in the thymus. (A)** CD4/CD8 profiles of TCR⁻ thymocytes in E2Δ^{ISP}CXCR4^{Tg} and E2Δ^{DP}CXCR4^{Tg} mice. Numbers above each box denote frequency of indicated population. **(B)** CXCR4^{Tg} expression significantly decreases the percentage of TCR⁻CD8⁺ cells escaping from the thymus into the LNs of E2Δ^{DP} mice. Bar graph represents 100% of TCR⁻CD8⁺ T cells in individual E2Δ^{DP} and E2Δ^{DP}CXCR4^{Tg} mice, and displayed are their relative in vivo distribution between thymus and LN. **(C)** CXCR4^{Tg} expression significantly diminishes numbers of peripheral TCR⁺CD8⁺ LN T cells in E2Δ^{ISP}and E2Δ^{DP} mice. **(D)** CCR7 deficiency does not significantly affect the percentage of TCR⁻CD8⁺ T cells escaping from the thymus (Thy) into the periphery (LN + Spleen) of E2Δ^{DP} mice. Bar graph represents 100% of TCR⁻CD8⁺ T cells in individual E2Δ^{DP} and E2Δ^{DP}CCR7$^{-/-}$ mice, and displayed are their relative distribution in vivo between thymus and LN + spleen. **(E)** CD69^{Tg} expression does not alter CXCR4 and CCR7 aberrant expression on preselection E2Δ^{ISP} thymocytes. Profiles of CXCR4, CCR7, and CD69 on TCRβ⁻CD4⁻CD8⁺ thymocytes from B6, E2Δ^{ISP}, and E2Δ^{ISP}CD69^{Tg} mice. **(F)** Immunofluorescence showing positioning in the thymic cortex or medulla of DP and SP thymocytes in B6 and SDF$^{\Delta TEC}$ mice. The thymic medulla is identified by K14 staining (white), and DP thymocytes are identified by Rorγt⁺ staining (green) in left panels and by their yellow appearance in right panels. DP thymocytes (Rorγt⁺CD4⁺CD8⁺) are present in the cortex but not the medulla. **(G)** Thymocyte profiles from B6, SDF$^{\Delta TEC}$S1P$_1^{Tg}$, and S1P$_1^{Tg}$ mice. CD4/CD8 profiles of total thymus from B6, SDF$^{\Delta TEC}$ S1P$_1^{Tg}$, and S1P$_1^{Tg}$ mice. Numbers above each box within the plot indicate frequencies of different thymocyte subsets. **(H)** CD4 versus CD8 profile on Thy1⁺TCRγδ⁻TCRβ⁻ spleen cells from SDF$^{\Delta TEC}$S1P$_1^{Tg}$ mice. Data are from two to four experiments with 3–13 mice per genotype (A–C) or four experiments with 4–10 mice per genotype (D and E) and are representative of three mice per genotype (H). Mean ± SEM are shown. **, $P < 0.01$ determined by Student's *t* test.

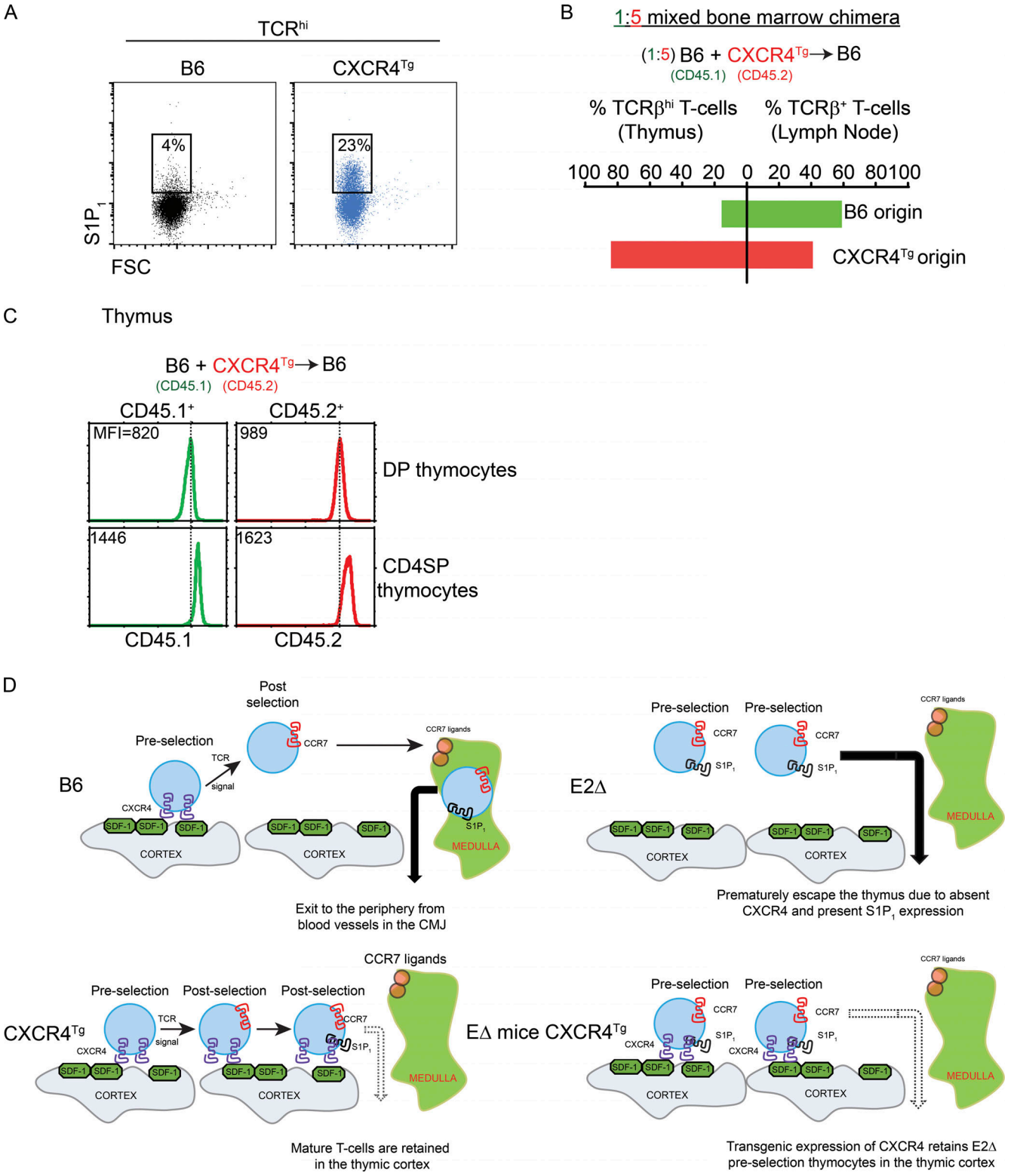

Figure S5. **Transgenic CXCR4 expression increases thymic residency time. (A)** $S1P_1$ expression on $TCR\beta^{hi}$ thymocytes from B6 and $CXCR4^{Tg}$ mice. Numbers within plots indicate the frequency of $TCR\beta^{hi}S1P_1^{+}$ thymocytes. **(B)** Bar graph displaying the frequency in (1:5) B6+$CXCR4^{Tg}$->B6 irradiation mixed bone marrow chimeras of B6 origin (CD45.1) versus $CXCR4^{Tg}$ (CD45.2) origin $TCR\beta^{hi}$ cells in the thymus and LNs. **(C)** CD45.1 and CD45.2 MFI on B6 and $CXCR4^{Tg}$ origin DP and CD4SP thymocytes from B6+$CXCR4^{Tg}$->B6 irradiation mixed bone marrow chimeras. Numbers within the plot indicate MFI of CD45 expression on the indicated thymocyte subsets. Data are representative from two to five experiments with five to nine mice per genotype. **(D)** Schematic model pictorially depicting the role of chemokine receptors (CXCR4, CCR7, and $S1P_1$) in thymocyte migration in the thymus of B6, $CXCR4^{Tg}$, E2Δ, and E2Δ $CXCR4^{Tg}$ mice.